

INSTITUTE FOR FUSION STUDIES

DE-FG05-80ET-53088-737

IFSR #737

Multiplicity of Low-Shear Toroidal Alfvén Eigenmodes

J. CANDY

JET Joint Undertaking
Abingdon, Oxfordshire OX14 3EA, UK

B.N. BREIZMAN and J.W. Van Dam

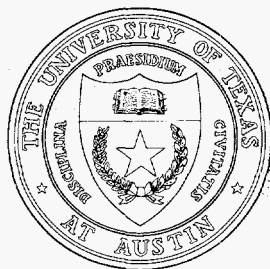
Institute for Fusion Studies
The University of Texas at Austin
Austin, Texas 78712 USA and

T. OZEKI

Naka Fusion Research Establishment
Japan Atomic Energy Research Institute
Naka-machi, Naka-gun, Ibaraki-ken 311-01, Japan

January 1996

THE UNIVERSITY OF TEXAS



RECEIVED
MAR 05 1997
OSTI

MASTER

AUSTIN

DISTRIBUTION OF THIS DOCUMENT IS UNLIMITED

8

DISCLAIMER

**Portions of this document may be illegible
in electronic image products. Images are
produced from the best available original
document.**

Multiplicity of low-shear toroidal Alfvén eigenmodes

J. Candy

JET Joint Undertaking, Abingdon, Oxfordshire OX14 3EA, UK

B.N. Breizman^{a)} and J.W. Van Dam

Institute for Fusion Studies, The University of Texas at Austin

Austin, Texas 78712 USA

and

T. Ozeki

Naka Fusion Research Establishment, Japan Atomic Energy Research Institute

Naka-machi, Naka-gun, Ibaraki-ken 311-01, Japan

Abstract

An enlarged spectrum of ideal toroidal Alfvén eigenmodes is demonstrated to exist within a toroidicity-induced Alfvén gap when the inverse aspect ratio is comparable to or larger than the value of the magnetic shear. This limit is appropriate for the low-shear region in most tokamaks, especially those with low aspect ratio. The new modes may be destabilized by fusion-product alpha particles more easily than the standard toroidal Alfvén eigenmodes.

DISCLAIMER

This report was prepared as an account of work sponsored by an agency of the United States Government. Neither the United States Government nor any agency thereof, nor any of their employees, makes any warranty, express or implied, or assumes any legal liability or responsibility for the accuracy, completeness, or usefulness of any information, apparatus, product, or process disclosed, or represents that its use would not infringe privately owned rights. Reference herein to any specific commercial product, process, or service by trade name, trademark, manufacturer, or otherwise does not necessarily constitute or imply its endorsement, recommendation, or favoring by the United States Government or any agency thereof. The views and opinions of authors expressed herein do not necessarily state or reflect those of the United States Government or any agency thereof.

^{a)}Also at Budker Institute of Nuclear Physics, Novosibirsk 630090, Russia

Recent studies^{1,2} have shown the existence in a tokamak plasma of two "core-localized" modes, which are low-shear versions of the ideal toroidal Alfvén eigenmodes (TAE). The significance of these modes is that, being low-shear, they are located near the magnetic axis where, in an ignited plasma, the population of fusion alpha particles is strongly peaked. Hence these modes could affect alpha particle confinement through TAE instability in deuterium-tritium experiments. Furthermore, in advanced tokamak reversed-shear operation, the region of low shear may be radially broadened, leading to the possibility of the prevalence of such TAE modes.

The previous theoretical demonstrations of the existence of the two core-localized modes relied on the assumption of the inverse aspect ratio being much smaller than the value of the magnetic shear: i.e., $\epsilon \ll s$, where $\epsilon = r/R_0$ is the inverse aspect ratio, with r the plasma minor radius and R_0 the major radius at the magnetic axis, and $s = (r/q)(dq/dr)$ is the magnetic shear, with $q(r)$ the safety factor. When this inequality holds, there are two distinct spatial scale lengths, which allows an analytic boundary-layer type of solution by means of asymptotic matching. However, for typical tokamak parameters, the ordering $\epsilon \approx s$ holds in the core region of the plasma. Moreover, for low-aspect-ratio spherical tokamaks, in which there is much interest recently,³ the corresponding ordering is likely to be $\epsilon \gg s$. In either of these cases, the previous solution procedure breaks down.

In the present Letter, we show how to solve the low-shear TAE equations in the realistic limit of $\epsilon \geq s$. Significantly, we find the result that there exists a large spectrum of core-localized modes within a given Alfvén gap, instead of only two. Due to their broadened width, we expect that these multiple modes can be more easily destabilized by energetic alpha particles than can the standard toroidal Alfvén eigenmodes, ideal or nonideal.

The linearized ideal magnetohydrodynamic equation for shear Alfvén waves can be re-

duced, for the case of high toroidal mode number, to

$$\mathbf{B} \cdot \nabla \left(\frac{1}{B^2} \nabla \cdot B^2 \nabla_{\perp} \frac{1}{B^2} \mathbf{B} \cdot \nabla \Phi \right) + \nabla \cdot \left(\frac{\omega^2}{v_A^2} \nabla_{\perp} \Phi \right) = 0. \quad (1)$$

In this work we consider the zero-pressure limit in order to clarify the analysis. Coupling to the higher frequency compressional Alfvén branch is neglected, which leaves Eq. (1) as a single scalar equation for the electrostatic potential Φ . The notation is that ω is the mode frequency, v_A the Alfvén speed, and \mathbf{B} the equilibrium magnetic field.

To analyze Eq. (1), introduce flux-type large-aspect-ratio coordinates (r, θ, ζ) , which are related to the usual cylindrical coordinates (R, φ, Z) centered on the toroidal axis of symmetry as follows⁴:

$$\begin{aligned} R &= R_0 + r \cos \theta - \Delta(r) + r\eta(r)(\cos 2\theta - 1) \\ \varphi &= -\zeta \end{aligned} \quad (2)$$

$$Z = r \sin \theta + r\eta(r) \sin 2\theta$$

with $\eta(r) = (\varepsilon + \Delta')/2$, where Δ' is the radial derivative of the Shafranov shift of a magnetic flux surface. In this nonorthogonal basis, the equilibrium magnetic field has the contravariant components

$$(B^r, B^{\theta}, B^{\zeta}) = \left(0, \frac{I}{qR^2}, \frac{I}{R^2} \right) \quad (3)$$

where $I = R^2 \cdot \nabla \zeta$ is a flux quantity related to the plasma current. Decompose the potential into poloidal harmonics as $\Phi = \exp(in\zeta - i\omega t) \sum_m \phi_m(r) \exp(-im\theta)$, with m and n the toroidal and poloidal mode numbers. In the large-aspect-ratio and low-shear limit, the mode is localized in the vicinity of a single Alfvén gap at $r = r_m$, where r_m is given by $q(r_m) = (m + 1/2)/n$, with q the safety factor, and consists of only two harmonics ϕ_m and ϕ_{m+1} . Then we can rewrite Eq. (1) as a pair of coupled equations:

$$\begin{aligned}
& \frac{d}{dy} \left[\Omega^2 - \left(y + \frac{1}{2} \right)^2 \right] \frac{d\phi_m}{dy} - \frac{1}{s^2} \left[\Omega^2 - \left(y + \frac{1}{2} \right)^2 \right] \phi_m \\
& = -\eta \frac{d^2 \phi_{m+1}}{dy^2} - \left(\frac{\varepsilon - \Delta'}{s} \right) \frac{d\phi_{m+1}}{dy} - \left(\frac{\Delta'}{2s^2} \right) \phi_{m+1}
\end{aligned} \tag{4}$$

$$\begin{aligned}
& \frac{d}{dy} \left[\Omega^2 - \left(y - \frac{1}{2} \right)^2 \right] \frac{d\phi_{m+1}}{dy} - \frac{1}{s^2} \left[\Omega^2 - \left(y - \frac{1}{2} \right)^2 \right] \phi_{m+1} \\
& = -\eta \frac{d^2 \phi_m}{dy^2} + \left(\frac{\varepsilon - \Delta'}{s} \right) \frac{d\phi_m}{dy} - \left(\frac{\Delta'}{2s^2} \right) \phi_m
\end{aligned} \tag{5}$$

Here, $\Omega = \omega/2\omega_0$ is the normalized frequency, with $\omega_0 = v_A(r_m)/2q(r_m)R_0$ the frequency at the center of the gap, and $y = n[q - q(r_m)]$ is the radial coordinate.

Notice the first-derivative terms on the right-hand sides of both Eqs. (4) and (5). These terms were not included in the treatment of Ref. 2. In the $\varepsilon \geq s$ limit considered here, these terms are significant, broadening the radial mode width.

In the core plasma region where we focus our attention, the shear, inverse aspect ratio, and Shafranov shift gradient are all naturally small: i.e., $s, \varepsilon, \Delta' \ll 1$. For applicability to realistic tokamaks, however, we wish to seek the solution when the ratios ε/s and Δ'/s are arbitrary compared to unity. Note from the definition $\Delta' \equiv \varepsilon(\ell_i/2 + \beta_p)$, with ℓ_i the internal inductance and β_p the poloidal beta, that we have the relationship $\Delta' = c\varepsilon$ in the zero-beta limit, where the proportionality constant has the value $c = 0.25$ in the case when the radial profile of the current is flat.

Therefore, dropping small $\mathcal{O}(s)$ terms but retaining terms of $\mathcal{O}(\varepsilon/s)$, we can rewrite the coupled eigenmode equations, Eqs. (4) and (5), in the following simplified form:

$$z(\ddot{S} - S) + (1 - \varepsilon^* c_1)\dot{S} + \varepsilon^*(1 - g)\ddot{A} + \varepsilon^*(g + c_0)A = 0 \tag{6}$$

$$z(\ddot{A} - A) + (1 + \varepsilon^* c_1)\dot{A} - \varepsilon^*(1 + g)\ddot{S} + \varepsilon^*(g - c_0)S = 0. \quad (7)$$

Here, $S = \phi_m + \phi_{m+1}$ and $A = \phi_m - \phi_{m+1}$ are symmetric and antisymmetric combinations of the coupled mode harmonics, with $\dot{S} \equiv dS/dz$ and so forth, where $z = y/s$ is the scaled radial coordinate in the low-shear regime. We have replaced the frequency according to $\Omega^2 = 1/4 + \eta g$, where g measures the shift of the frequency away from the center of the Alfvén gap; the normalization is such that the values $g = \pm 1$ correspond, respectively, to the upper and lower ideal Alfvén continua. Nonsingular eigenmodes will exist within the gap for discrete values of g in the interval $-1 < g < +1$. The constants defined by $c_0 = c/(1 + c) < 1$ and $c_1 = 2(1 - c)/(1 + c)$ assume the values $c_0 = 0.2$ and $c_1 = 1.2$ for uniform current. Equations (6) and (7) are to be solved with the boundary conditions that the wave functions vanish at large argument. Thus, for a given Shafranov shift, the problem is reduced in the zero-beta limit to obtaining the eigenvalue g as a function of only a single parameter $\varepsilon^* \equiv \eta/s = \varepsilon(1 + c)/2s$.

It is straightforward to integrate Eqs. (6) and (7) numerically. Results are presented in Fig. 1, for the flat-current case ($c = 0.25$). It is also possible to obtain an approximate analytic solution in the large- ε^* limit, which will facilitate the interpretation of certain interesting features of these results.

Consider Eqs. (6) and (7) for the case when $\varepsilon^* \gg 1$. This allows a long wavelength solution with the ordering $\ddot{S} \ll S \sim \varepsilon^* \ddot{S}$, and similarly for $A(z)$. We first consider the case when $g = c_0 - \lambda$, with $\lambda \sim \mathcal{O}(1/\varepsilon^*) \ll c_0$. Then Eqs. (6) and (7) reduce to

$$-zS - \varepsilon^* c_1 \dot{S} + 2c_0 \varepsilon^* A \cong 0 \quad (8)$$

$$-zA + \varepsilon^* c_1 \dot{A} - \varepsilon^*(1 + c_0)\ddot{S} - \lambda \varepsilon^* S \cong 0. \quad (9)$$

All the terms in Eqs. (8) and (9) are the same order, with $|A/S| \sim \mathcal{O}(1/\sqrt{\varepsilon^*}) < 1$. These two equations can be combined into one harmonic-oscillator-type equation for the symmetric

eigenfunction S ,

$$\varepsilon^{*2} [c_1^2 - 2c_0(1 + c_0)] \tilde{S} + [(\varepsilon^* c_1 - 2c_0 \varepsilon^{*2} \lambda) - z^2] S \cong 0, \quad (10)$$

from which we immediately obtain the eigenvalues

$$g_\ell^{(+)} \cong c_0 + \frac{1}{2c_0 \varepsilon^*} [-c_1 + (2\ell + 1)\sqrt{c_1^2 - 2c_0(1 + c_0)}], \quad \ell = 0, 1, 2, 3, \dots \quad (11)$$

The corresponding wave functions are $S(z) = \exp(-\xi^2/2)H_\ell(\xi)$, where $H_\ell(\xi)$ are the Hermite polynomials, with argument $\xi = z/\sqrt{\varepsilon^*} [c_1^2 - 2c_0(1 + c_0)]^{1/4}$. Proceeding in a similar manner for the case when $g = -c_0 + \lambda$, we find that now the antisymmetric wave function is dominant, $|A/S| \sim \mathcal{O}(\sqrt{\varepsilon^*}) > 1$, and the eigenvalues are given by

$$g_{\ell+1}^{(-)} \cong -c_0 - \frac{1}{2c_0 \varepsilon^*} [c_1 + (2\ell + 1)\sqrt{c_1^2 - 2c_0(1 + c_0)}], \quad \ell = 0, 1, 2, 3, \dots \quad (12)$$

The validity of Eqs. (11) and (12) requires small radial quantum number, i.e., $\ell \ll \varepsilon^* c_0^2 / c_1$.

Continuing our analytical exploration, we note that by means of Fourier transformation the full set of Eqs. (6) and (7) for the low-shear eigenmodes can be recast, without any approximation, as a single second-order equation:

$$\left[\frac{d^2}{dk^2} - V_\pm(k) \right] \Psi_\pm(k) = 0. \quad (13)$$

Here the potential V_\pm is given by

$$-V_\pm(k) = \varepsilon^{*2}(g^2 - P^2 - c_1^2 Q^2) \pm \varepsilon^* c_1 \left(Q' - \frac{QP'}{P \pm g} \right) + \frac{P''}{2(P \pm g)} - \frac{3}{4} \left(\frac{P'}{P \pm g} \right)^2 \quad (14)$$

with $Q(k) = k/(1 + k^2)$, $P(k) = (c_0 - k^2)/(1 + k^2)$, and $P' = dP/dk$. Equation (13) is valid for either wavefunction Ψ_+ or Ψ_- , defined by

$$\begin{pmatrix} \Psi_+(k) \\ \Psi_-(k) \end{pmatrix} = \sqrt{\frac{1 + k^2}{P \pm g}} \int_{-\infty}^{+\infty} dz \exp(ikz) \begin{pmatrix} S(z) \\ A(z) \end{pmatrix} \quad (15)$$

The advantage of the Fourier transformation is that it reduces the order of the eigenmode equations. Their numerical solution in k -space is therefore easier than in real z -space. Analytically, the problem is simplified because it is reduced to the consideration of a Schrödinger-type equation, whose treatment is familiar. For instance, the large- k form of the potential,

$$V_{\pm}(k) \xrightarrow{|k| \rightarrow \infty} \varepsilon^{*2} (1 - g^2) \quad (16)$$

indicates that the solution is asymptotically well-behaved, $\Psi_{\pm} \rightarrow \exp(\varepsilon^* \sqrt{1 - g^2} |k|)$, as long as the frequency does not enter the Alfvén continuum. Also, the value of the potential at $k = 0$, which is given by

$$V_{\pm}(0) = - \left[\varepsilon^{*2} (g^2 - c_0^2) \pm \varepsilon^* c_1 - \frac{(1 + c_0)}{(c_0 \pm g)} \right] \quad (17)$$

must be negative for the existence of bound-state solutions. In the $\varepsilon^* \gg 1$ limit, this requires that $|g| > c_0$ be generally satisfied in order to have nonsingular solutions, leading to an interior spectral “forbidden zone” of width $\Delta g = 2c_0$. An exception occurs when the value of $|g|$ is very close to c_0 , in which case the $\mathcal{O}(\varepsilon^*)$ term in Eq. (17) contributes to making the potential V_+ deeper than V_- and thus allowing an extra solution for the Ψ_+ wavefunction. Finally, the WKB quantization condition $\oint dk \sqrt{V_{\pm}(k)} = (2\ell + 1)\pi$ can be used to obtain the eigenvalues when the potential is slowly varying. In the $\varepsilon^* \gg 1$ limit, the ordering $k^2 \ll 1$ for the bound-state turning points is appropriate, and we can then obtain the approximate expression

$$g_{\ell}^2 \cong c_0^2 + (2\ell + 1) \frac{1}{\varepsilon^*} \sqrt{c_1^2 - 2c_0(1 + c_0)} \quad (18)$$

which is fairly accurate even when ε^* is not very large. The validity of this WKB result requires $\ell \gg 1$. However, the number of modes is limited by $\ell < \varepsilon^* c_1^2$, since $g^2 < 1$.

Let us now compare the analytical results with the exact numerical results for the sake of interpretation. The approximate analytical results of Eqs. (11), (12), and (18) indicate that a multiplicity of eigenmodes, indexed by the non-negative radial mode number ℓ , exists when

$\epsilon^* \geq 1$. This feature is exhibited by the numerical results in Fig. 1. From Ref. 2 we already know that in the $\epsilon^* \ll 1$ limit, there exists a core-localized eigenmode whose frequency is near the bottom of the Alfvén gap and whose mode structure has the polarization corresponding to that of the symmetric function $S(z)$ or $\Psi_+(k)$, and there is another solution whose frequency is near the top of the Alfvén gap and whose mode structure has the polarization corresponding to that of the antisymmetric function $A(z)$ or $\Psi_-(k)$. In the zero-beta limit, the existence of the upper core-localized mode was found² to require $\epsilon^* > s(1+c)/2(1+2c)$, which, however, is not exhibited in Fig. 1 since this condition is outside the scaling adopted in the present analysis. The lower core-localized mode has no corresponding condition for existence. As the value of ϵ^* increases above unity, more eigenmodes enter the spectrum one by one. Figure 1 shows only the first seven eigenvalues for each polarization. In general, as the inverse aspect ratio increases, the eigenvalues for the modes with antisymmetric polarization (higher frequency) slowly decrease toward $+c_0$ from above, and the eigenvalues for the modes with symmetric polarization (lower frequency) slowly increase toward $-c_0$ from below. The one exception is the lowest-order ($\ell = 0$) symmetric mode, the branch which in the $\epsilon^* \rightarrow 0$ limit goes over to the usual ideal TAE mode. This mode may be understood by noticing that Eq. (11) yields a root just below $g = c_0$ if $\ell = 0$, whereas Eq. (12) has no corresponding root above $g = -c_0$. This behavior is related to the difference in the depth of the Fourier-space potential well, remarked upon earlier. The $c_1/2c_0\epsilon^*$ term in Eqs. (11) and (12), which causes this difference, becomes less significant as the radial quantization number ℓ increases, so that the higher-order eigenvalues tend toward equal but opposite pairs, as in Eq. (18). At large ϵ^* we find fairly good quantitative agreement with the numerical eigenvalues g_ℓ in Fig. 1 when we use the real-space estimates of Eqs. (11) and (12) for $\ell = 0, 1$ and the WKB estimate of Eq. (18) for $\ell > 1$. Also notice that the Alfvén gap enlarges with ϵ^* , whereas the spacing in frequency of the multiple modes is constant for a given value of the shear.

The results found here have several intriguing implications. First, it is now clear that there are not merely two TAE modes in the low-shear region, but instead a multiple spectrum. The lowest-order symmetrically polarized mode connects to the lower-frequency core-localized mode (which corresponds to the usual TAE), in the limit when the inverse aspect ratio is small compared to the magnetic shear. The lowest-order antisymmetric mode corresponds to the upper-frequency core-localized mode of Ref. 2 in the same small but nonzero inverse aspect ratio limit. However, in the more realistic case when the inverse aspect ratio is comparable to or larger than the magnetic shear (appropriate, respectively, for the central region of a usual tokamak or a spherical tokamak), the spectrum is significantly enlarged and there exists a multiplicity of core-localized modes. This feature may facilitate the consideration of low-shear modes for the purpose of investigating Alfvén-type instability properties in present-day deuterium/tritium experiments.⁵ Non-ignition experiments that can use external antennae to excite and study Alfvén eigenmodes⁶ may be able to observe this multiplicity of core-localized modes. Two-dimensional codes for TAE stability analysis of fusion plasmas should also confirm this result.

Another significant implication is that we expect these multiple core-localized modes, due to their broadened width, to be more strongly destabilized by energetic alpha particles than the standard ideal or nonideal toroidal Alfvén eigenmodes. For the standard ideal TAE mode,⁷ located in the finite-shear, i.e., $s = \mathcal{O}(1)$, region, the outer radial mode width Δr of a poloidal harmonic is $(\Delta r)_{\text{out}} \approx r/m$, although most of the wave energy is concentrated in a narrow inner width that scales as $(\Delta r)_{\text{in}} \approx (\varepsilon/s)(r/m)$. Contrast this with the low-shear modes found here, whose radial mode width scales as $\Delta r \approx \sqrt{\varepsilon/s} (r/m)$, which exceeds either the inner or outer TAE mode width since in the low-shear region the local value of ε/s is typically high. Larger mode width implies stronger drive. (A method for calculating the drive in the low-shear limit has been described recently.⁸) Large mode width also implies that the modes are relatively insensitive to nonideal effects,^{9,10} which are small scale, and

also to finite orbit width effects.¹¹ Although thermal pressure gradient effects should be checked, which for the usual TAE mode can shift its frequency into the continuum and lead to strong dissipation,¹²⁻¹⁴ we expect that they may not be too significant since the lowest-order eigenfrequencies are not close to either edge of the gap. We expect, therefore, that this multiplicity of core-localized modes could be more robustly unstable than the usual TAE or the kinetic TAE modes.

We appreciate Dr. Emilia Solano for prompting us to think about spherical tokamaks. Support and hospitality are gratefully acknowledged by one author (JVD) during his visit at the Japan Atomic Energy Research Institute, and by another (BNB) during his visit at the JET Joint Undertaking. This work was also supported by the U.S. Department of Energy under Contract No. DE-FG03-96ER-54346.

REFERENCES

- ¹G.Y. Fu, Phys. Plasmas **2**, 1029 (1995).
- ²H.L. Berk, J.W. Van Dam, D. Borba, J. Candy, G.T.A. Huysman, and S. Sharapov, Phys. Plasmas **2**, 3401 (1995).
- ³A. Sykes, Plasma Phys. Control. Fusion **36**, B93 (1994); A. Sykes *et al.*, "The START Spherical Tokamak," in: *Proc. Intl. Conf. on Plasma Physics and Control. Nucl. Fusion* (to be published by International Atomic Energy Agency, Vienna, 1995), paper IAEA-CN-60/A5-II-5.
- ⁴J.D. Meiss and R.D. Hazeltine, Phys. Fluids B **2**, 1563 (1990).
- ⁵G.Y. Fu *et al.*, Phys. Rev. Lett. **75**, 2336 (1995).
- ⁶A. Fasoli *et al.*, Phys. Rev. Lett. **75**, 645 (1995).
- ⁷See, for example, M.N. Rosenbluth, H.L. Berk, J.W. Van Dam, and D.M. Lindberg, Phys. Fluids B **4**, (1992) 2189.
- ⁸B.N. Breizman and S. Sharapov, Plasma Phys. Control. Fusion **37**, 1057 (1995).
- ⁹R.R. Mett and S.M. Mahajan, Phys. Fluids B **4**, 2885 (1992).
- ¹⁰J. Candy and M. N. Rosenbluth, Phys. Plasmas **1**, 356 (1994).
- ¹¹H.L. Berk, B.N. Breizman, and H. Ye, Phys. Lett. A **162**, 475 (1992).
- ¹²L. Chen, "On resonant excitation of high-n magnetohydrodynamic modes by energetic/alpha particles in tokamaks," in: *Theory of Fusion Plasmas*, ed. J. Vaclavik, F.

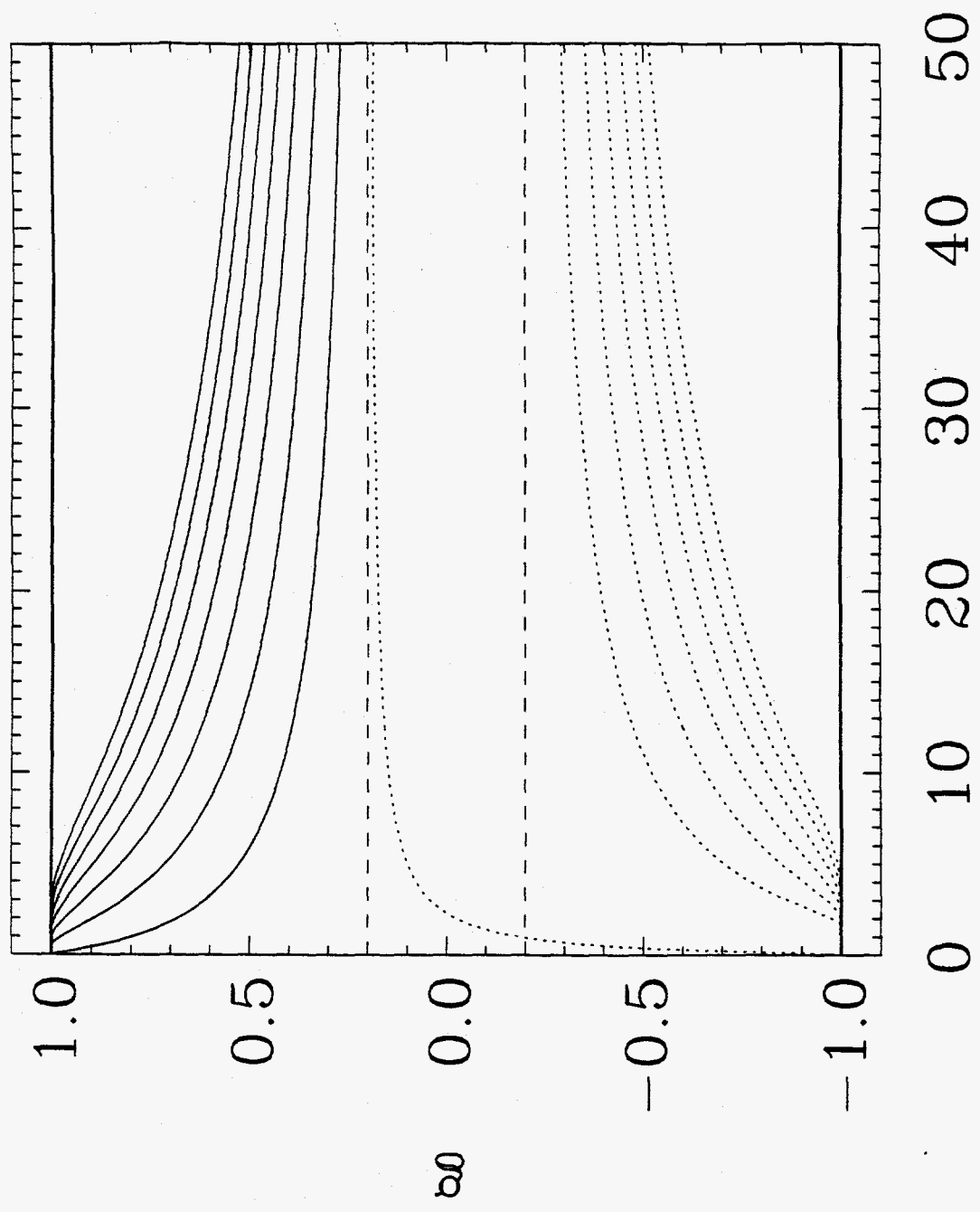
Troyon, and E. Sindoni (Editrice Compositori Societa Italiana di Fisica, Bologna, 1989), p. 327.

¹³G.Y. Fu and C.Z. Cheng, Phys. Fluids B **2**, 985 (1990).

¹⁴F. Zonca and L. Chen, Phys. Fluids B **5**, 3668 (1993).

FIGURE CAPTIONS

FIG. 1. Spectrum of values of the eigenfrequency shift g as a function of the inverse aspect ratio parameter ε^* for the first seven symmetric (solid curves) and antisymmetric (dashed curves) eigenmodes, for the flat-current case ($c_0 = 0.2$). No modes exist within the interior "forbidden zone" demarcated by the two horizontal lines (large dashes) at $g = \pm c_0$, except the lowest-order symmetric mode.



$$\epsilon^* = \epsilon/s$$

Fig. 1